



HAL
open science

Mother-plant-mediated pumping of zinc into the developing seed

Lene Irene Olsen, Thomas Hansen, Camille Larue, Jeppe Thulin Osterberg, Robert Hoffmann, Johannes Liesche, Ute Kramer, Suzy Surblé, Stéphanie Cadarsi, Vallerie Ann Samson, et al.

► **To cite this version:**

Lene Irene Olsen, Thomas Hansen, Camille Larue, Jeppe Thulin Osterberg, Robert Hoffmann, et al.. Mother-plant-mediated pumping of zinc into the developing seed. *Nature Plants*, 2016, 2 (5), 10.1038/nplants.2016.36 . hal-02325140

HAL Id: hal-02325140

<https://hal.science/hal-02325140>

Submitted on 10 Nov 2020

HAL is a multi-disciplinary open access archive for the deposit and dissemination of scientific research documents, whether they are published or not. The documents may come from teaching and research institutions in France or abroad, or from public or private research centers.

L'archive ouverte pluridisciplinaire **HAL**, est destinée au dépôt et à la diffusion de documents scientifiques de niveau recherche, publiés ou non, émanant des établissements d'enseignement et de recherche français ou étrangers, des laboratoires publics ou privés.

Mother plant-mediated pumping of zinc into the developing seed

Lene Irene Olsen^{1,2}, Thomas H. Hansen², Camille Larue^{3,4}, Jeppe Thulin Østerberg^{1,2}, Robert D. Hoffmann^{1,2}, Johannes Liesche^{2,5}, Ute Krämer³, Suzy Surblé⁶, Stéphanie Cadarsi⁴, Vallerie Ann Samson⁷, Daniel Grolimund⁷, Søren Husted² and Michael Palmgren^{1,2,8*}

1 Insufficient intake of zinc and iron from a cereal-based diet is one of the causes of “hidden hunger” (micronutrient deficiency), which affects some two billion people^{1,2}. Identifying a limiting factor in the molecular mechanism of zinc loading into seeds is an important step towards determining the genetic basis for variation of grain micronutrient content and developing breeding strategies to improve this trait³. Nutrients are translocated to developing seeds at a rate that is regulated by transport processes in source leaves, in the phloem vascular pathway, and at seed sinks. Nutrients are released from a symplasmic maternal seed domain into the seed apoplasm surrounding the endosperm and embryo by poorly understood membrane transport processes^{4–6}. Plants are unique among eukaryotes in having specific P1B-ATPase pumps for the cellular export of zinc⁷. In *Arabidopsis*, we show that two zinc transporting P1B-ATPases actively export zinc from the mother plant to the filial tissues. Mutant plants that lack both zinc pumps accumulate zinc in the seed coat and consequently have vastly reduced amounts of zinc inside the seed. Blockage of zinc transport was observed both at high and low external zinc supplies. The phenotype was determined by the mother plant and is thus due to a lack of zinc pump activity in the seed coat and not in the filial tissues. The finding that P1B-ATPases are one of the limiting factors controlling the amount of zinc inside a seed is an important step towards combating nutritional zinc deficiency worldwide.

In the quest to identify the membrane-bound transporters that deliver zinc into seeds, heavy metal-transporting P1B-ATPases, which belong to the family of P-type ATPases that actively transport ions and lipids across membranes, are promising candidates. In *Arabidopsis thaliana*, the P1B-ATPase subfamily consists of eight members, AtHMA1–8 (ref. 8). Whereas AtHMA2–4 transport divalent zinc and cadmium cations and AtHMA5–8 transport monovalent copper and silver cations, AtHMA1 has been implicated in the transport of a number of different cations including copper, silver, zinc and cadmium^{9,10}. AtHMA3 is localized to the tonoplast and is involved in detoxification by sequestering excess amounts of zinc and cadmium into the vacuole¹¹. AtHMA2 and AtHMA4 are structurally very similar to each other and have overlapping functions. Whereas the *hma2* and *hma4* single mutants have wild-type growth rates, the *hma2,hma4* double mutant shows a stunted growth phenotype that can only be rescued by zinc supplementation. Also, the *hma2,hma4* double mutant does

not set seed, a phenotype mainly ascribed to a defect in pollen development¹². Both AtHMA2 and AtHMA4 have been localized to the plasma membrane and function as cellular zinc exporters^{12–14}. Their involvement in xylem loading of zinc in roots is well known. They are both expressed in the root pericycle and xylem parenchyma cells and mutants lacking functional AtHMA2 and AtHMA4 accumulate zinc in the pericycle and endodermal cell layers, and exhibit reduced root-to-shoot translocation of zinc^{12,13}. The finding that the zinc hyperaccumulator *Arabidopsis halleri* accumulates high levels of zinc in the shoot mainly because of the strongly enhanced expression of *AhHMA4*, caused by activating *cis*-regulatory mutations and gene copy number expansion¹⁵, emphasizes the role of HMA4 in the root-to-shoot translocation of zinc.

To test whether developing seeds depend on *AtHMA2* and *AtHMA4* for proper zinc unloading from the seed coat, we analysed the amount of zinc present in the maternal and filial parts of the seed, respectively, in wild-type and mutant seeds lacking functional *AtHMA2*, *AtHMA4*, or both. For this purpose, we developed an assay in which mature seeds are separated into seed coat (with the endosperm attached) and embryo fractions, and their respective metal contents are subsequently analysed by inductively coupled plasma mass spectrometry (ICPMS). All seeds used for this analysis were from plants grown side by side in soil watered with 3 mM ZnSO₄ twice a week, as these conditions were needed for the *hma2,hma4* double mutant to set seed. At this relatively high zinc supply, trafficking of zinc to the shoot did not differ between genotypes (Supplementary Fig. 1). We determined the total amounts of zinc, magnesium, phosphorus and manganese in batches of ten mature seeds, either intact or separated into seed coat and embryo fractions, using ICPMS. This revealed that the content of the different genotypes or between the content of intact seeds and the combined content of separated seeds for the tested elements showed little variation (Supplementary Fig. 2). As there was no difference between the weight of seeds of different genotypes and the combined weight of their separated parts (Supplementary Fig. 3a), loss of material during the separation procedure was negligible. However, the weight of any ten seeds was variable, which explains the variance seen for the total amounts of element. Instead of weighing samples before ICPMS, which could result in contamination, we used the ratio of seed coat weight to embryo weight as a reference point for normalizing data as it consistently was found to be very similar between and within genotypes (Supplementary Fig. 3b).

We found that in wild-type seeds most of the zinc was present in the embryo fraction (Fig. 1a). Conversely, in the *hma2,hma4* double

¹Centre for Membrane Pumps in Cells and Disease-PUMPKIN, Danish National Research Foundation, Denmark. ²Department of Plant and Environmental Sciences, University of Copenhagen, Thorvaldsensvej 40, DK-1871 Frederiksberg, Denmark. ³Department of Plant Physiology, Ruhr University Bochum, Bochum, Germany. ⁴ECOLAB, Université de Toulouse, CNRS, INPT, UPS, France. ⁵College of Life Sciences, Northwest A&F University, Yangling, China. ⁶LEEL, NIMBE-CEA-CNRS, Université Paris-Saclay, CEA Saclay, Gif-sur-Yvette Cedex, France. ⁷MicroXAS beamline, Swiss Light Source, Villigen, Switzerland. ⁸Institute of Environmental Medicine, Karolinska Institutet, SE-171 77 Stockholm, Sweden. *e-mail: palmgren@plen.ku.dk

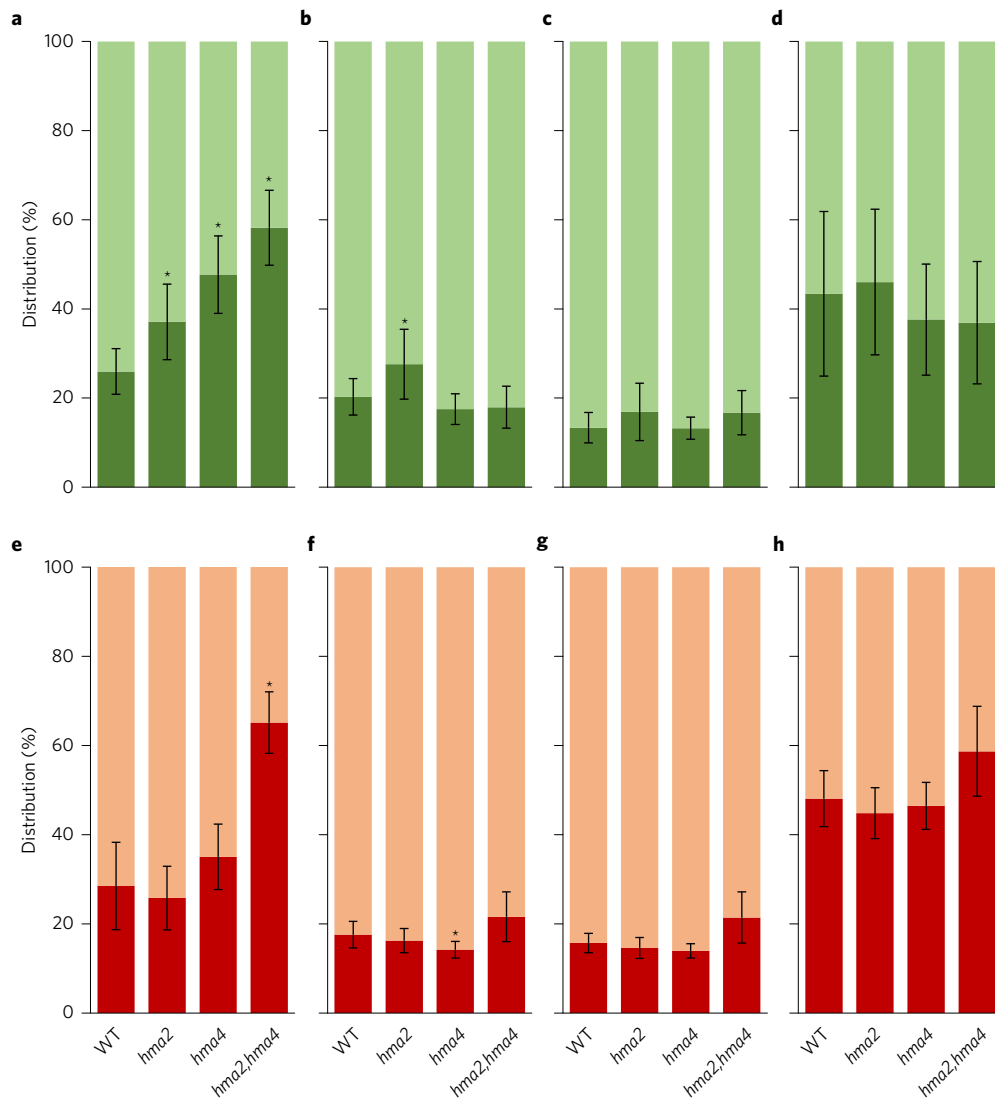


Figure 1 | The distribution of zinc is shifted from the embryo to the seed coat of mature *hma2,hma4* seeds. Microanalytical multi-elemental profiling of batches of ten seeds separated into seed coats and embryos. **a-h**, Distribution of elements in seeds from plants grown at high zinc supply (**a-d**) and plants grown at low zinc supply (**e-h**) (inflorescences of different genotypes had been grafted onto wild-type rootstocks). Bars represent the percentage of the total elemental content that is localized in the seed coat (dark green/red) and embryo (light green/red) fractions. **a,e**, Zinc; **b,f**, magnesium; **c,g**, phosphorus; and **d,h** manganese. Data are mean \pm s.d. of eight to ten replicates. Statistical analysis indicates significant difference from the wild type ($*p < 0.01$).

1 mutant, zinc accumulated in the seed coat fraction (Fig. 1a). In *hma2*
 2 and *hma4* single mutants, only slightly more zinc accumulated in the
 3 seed coat than the wild type, whereas the distribution of magnesium,
 4 phosphorus and manganese did not show the same shift (Fig. 1a-d).
 5 *hma2,hma4* double mutant plants did not develop seeds unless
 6 supplemented with a high amount of zinc (3 mM ZnSO₄ twice a
 7 week), but under these conditions overall zinc homeostasis of the
 8 plant may be perturbed. To make the *hma2,hma4* double mutant
 9 set seed under low zinc conditions, we grafted the mutant inflores-
 10 cences onto wild-type rootstock. When the resulting plants were
 11 grown under low external zinc conditions, *hma2,hma4* mutant
 12 inflorescences produced seeds, and, compared with the seeds of
 13 plants grown under high zinc conditions, contained a much lower
 14 zinc content (reduced from around 50–10 ng for 10 seeds,
 15 Supplementary Fig. 4). Under these conditions, seeds of *hma2*,
 16 *hma4* double mutant inflorescences accumulated zinc in the seed
 17 coat (Fig. 1e). This demonstrates that the *hma2,hma4* double
 18 mutant fails to direct zinc towards the embryo both under high
 19 and low external zinc supplies. By contrast, no shift in zinc

distribution was seen for the *hma2* and *hma4* single mutants at a
 20 low zinc supply (Fig. 1e). 21

To confirm that HMAs are required for export of zinc from
 22 the maternal to the filial parts of seeds, we employed micro-X-ray
 23 fluorescence (μ XRF) and micro-particle-induced X-ray emission
 24 (μ PIXE) coupled to micro-Rutherford backscattering spectroscopy
 25 (μ RBS) to obtain spatially resolved images of the distribution of
 26 zinc in wild-type and mutant seeds. μ PIXE/RBS also allows for
 27 quantification of elemental concentrations in the seed sections. 28
 For these experiments we obtained seeds from intact plants grown
 29 with zinc supplementation. Our analysis of μ XRF and μ PIXE/RBS
 30 maps of all together seven replicate sections imaged per genotype
 31 indicated that the spatial distribution of zinc was consistently
 32 altered in the *hma4* and *hma2,hma4* mutants compared with the
 33 wild type (Fig. 2, Supplementary Fig. 5 and Supplementary
 34 Table 1). In wild-type seeds, the distribution of elements was essen-
 35 tially as reported earlier^{16,17}. Iron was found to accumulate in the
 36 provascular strands, manganese surrounded these strands on the
 37 lower side of the cotyledons and calcium was enriched in the seed
 38 39

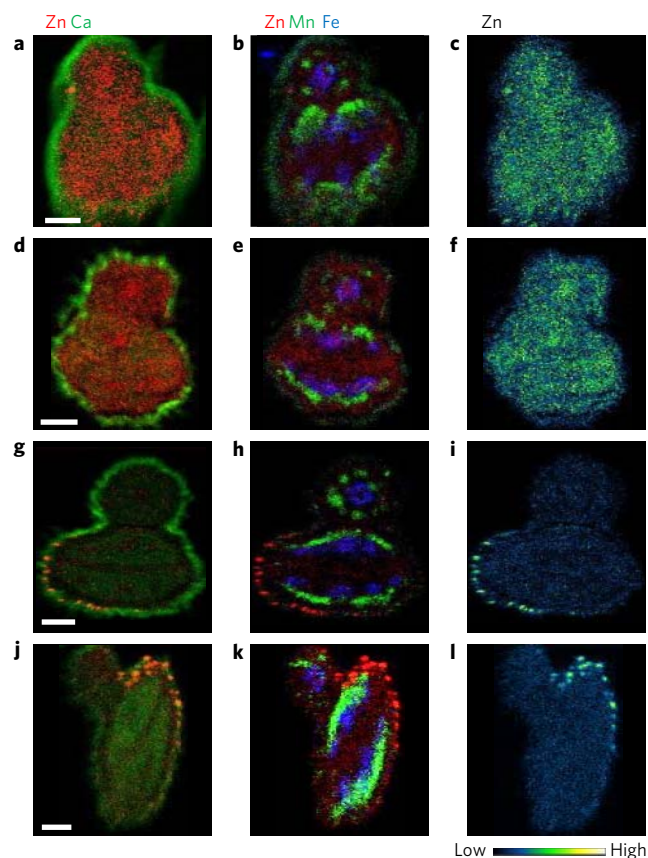


Figure 2 | Zinc accumulates in the seed coat of mature *hma4* and *hma2, hma4* mutant seeds. a–l, μ PIXE/RBS elemental profiles of transverse sections of seeds from wild-type (a–c), *hma2* mutant (d–f), *hma4* mutant (g–i) and *hma2,hma4* (j–l) double mutant plants grown at high zinc supply. a,d,g,j, Two-colour maps showing zinc (Zn) distribution in red and calcium (Ca) distribution in green. b,e,h,k, Three-colour maps showing zinc (Zn) distribution in red, manganese (Mn) distribution in green and iron (Fe) distribution in blue. c,f,i,l, Temperature colour maps displaying zinc distribution. Scale bars, 50 μ m.

1 coat and showed an even distribution in the embryo, as did zinc
2 (Fig. 2a–c). The pattern of zinc distribution in seeds of the *hma2*
3 single mutant was similar to that of the wild type (Fig. 2d–f). By
4 contrast, zinc distribution was far more uneven across sections of
5 seeds from both the *hma4* single mutant (Fig. 2g–i) and the
6 *hma2,hma4* double mutant (Fig. 2j–l). In these mutants, the zinc
7 signal was reduced in the embryo. By contrast, very high levels of
8 zinc accumulated in the seed coat, with the frequency of high-
9 intensity zinc hot spots gradually declining with increasing distance
10 from the hilum inside the seed coat. There were no consistent
11 changes in the distribution of other elements, such as calcium,
12 iron and manganese, among the replicate sections analysed (Fig. 2
13 and Supplementary Fig. 5).

14 To determine whether the ability to provide the embryo with zinc
15 was a maternal property, we performed crosses between wild-type or
16 *hma2,hma4* mother plants and wild-type or *hma2,hma4* pollen.
17 Wild-type plants always produced seeds with an even distribution
18 of zinc in the embryo, regardless of whether they had been fertilized
19 with *hma2,hma4* or wild-type pollen. By contrast, mother plants
20 with a *hma2,hma4* genotype always produced seeds that accumu-
21 lated zinc in the seed coat, regardless of the genotype of the
22 pollen (Figs. 3, 4 and Supplementary Table 2). This demonstrates
23 that the observed accumulation of zinc in the seed coat is due to the
24 lack of AtHMA2 and AtHMA4 in the seed coat itself. Taken together,

our ICPMS data in combination with μ XRF and μ PIXE/RBS
mapping of elemental distribution suggest that cellular export of
zinc towards the endosperm and embryo is blocked without the
combined function of AtHMA2 and AtHMA4 in the seed coat.

Genome-wide gene activity profiling suggests that *AtHMA2* and
AtHMA4 are both expressed in developing seeds¹⁸, (Supplementary
Fig. 6). To confirm the expression of *AtHMA2* and *AtHMA4* at this
location, we generated transgenic plants expressing β -glucuronidase
(GUS) and investigated the cell-specific expression of the GUS
reporter using whole-mount confocal imaging. The *AtHMA2* pro-
moter was active throughout the seed, including both the seed
coat and embryo, whereas *AtHMA4* was expressed in the innermost
cell layer of the seed coat surrounding the endosperm (the endo-
thelium), in the chalazal region, and also in the embryo (Fig. 5d,e).
This expression pattern was detected at all developmental stages
(data not shown). When green fluorescent protein (GFP) was
fused to the first half of AtHMA4 (HMA4-4TM-GFP) and the
resulting construct was expressed under the control of the *HMA4*
promoter in transgenic plants, we found GFP expression to be
strong in the endothelium (Fig. 5f,g). This is consistent with the
finding that, in the maternal tissues of developing seeds, *AtHMA4*
is specifically expressed in the seed coat endothelium.

On the basis of our results, we suggest a model in which
AtHMA2 and AtHMA4 are involved in the export of zinc from
the mother plant seed coat to the filial tissues. The phloem is a
long-distance vascular transport system in plants that transports
nutrients to reproductive tissues. In *Arabidopsis* seeds, the phloem
is symplastically connected to the seed coat. However, for nutrients
to proceed further into filial tissues, apoplastic barriers have to be
crossed, which requires transport across biological membranes⁴,
and for zinc export against the inside-negative membrane potential.
In the seed coat of the developing seed, an apoplastic barrier is
present between the outer and inner integument, as well as
between the inner integument and the endosperm, and between
the endosperm and the embryo⁴. Whereas *AtHMA2* was expressed
in all integuments, *AtHMA4* was mainly expressed in the innermost
layer of the seed coat, the endothelium. Thus, AtHMA4 is a prime
candidate for mediating the post-phloem translocation of zinc from
the seed coat and into the endosperm cavity. The importance of
AtHMA4 in this process is evident at a high zinc supply as, in the
hma4 mutant background, zinc accumulates in the seed coat, as
shown by both ICPMS and μ XRF/ μ PIXE. This phenotype is even
stronger in the *hma2,hma4* double mutant at both a high and low
zinc supply, which suggests that AtHMA2 also contributes to this
process. The fact that zinc is present in the embryo even in the
hma2,hma4 double mutant indicates that other transporters exist
in the seed coat that are able to export zinc into the endosperm
cavity. A similar phenomenon is seen in the root, where zinc is
loaded into the xylem even in the *hma2,hma4* double mutant^{12,13},
a transport that at least partially seems to be mediated by the
putative transporter AtPCR2 (ref. 19). However, this transport is
only efficient at high zinc concentrations, which suggests that
these secondary active transporters have a lower zinc affinity than
do AtHMA2/4.

AtHMA2 and AtHMA4 belong to the P1B-2 subgroup of heavy
metal ATPases, which are common in prokaryotes and plants but
absent in animals⁷. Plant cells have substantially higher inside-
negative membrane potentials than do animal cells²⁰, which may
be a reason why export of this micronutrient from plant cells
cannot be sustained by proton antiporters alone when zinc is limit-
ing, but requires the contribution of primary active transporters.
The AtHMA2/4 homologue in *Hordeum vulgare* (barley) is
HvHMA2, which functions as a plasma membrane-localized zinc
exporter²¹. Expression analysis of laser capture microdissected
developing barley grain showed that *HvHMA2* is predominantly
expressed in the nucellar projection transfer cells²², which

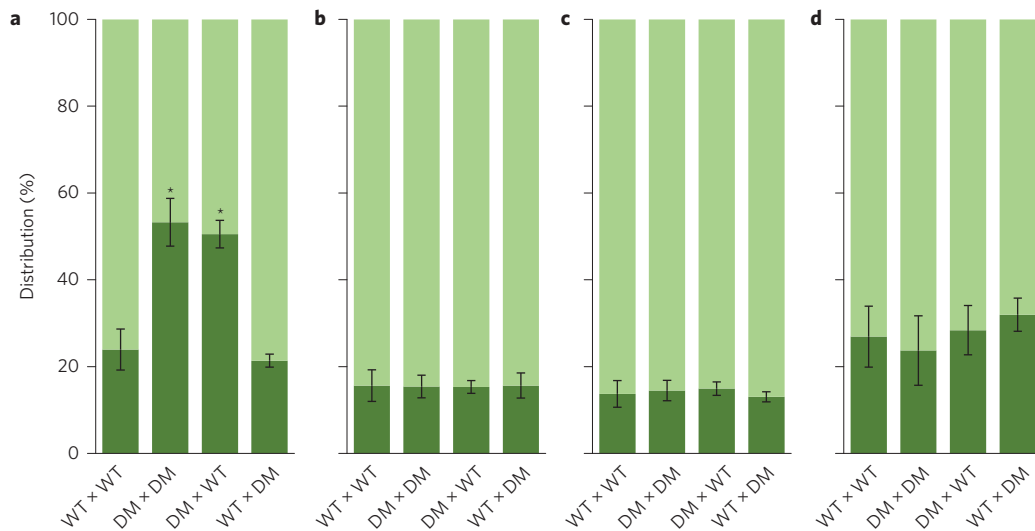


Figure 3 | Lack of zinc pumps in the seed coat but not in filial tissues blocks zinc loading into seeds. Microanalytical multi-elemental profiling of batches of ten seeds separated into seed coats and embryos. Bars represent the percentage of the total elemental content that is localized in the seed coat (dark green) and embryo (light green) fractions of seeds from crosses of plants grown at high zinc supply. Notations represent mother plant \times pollen donor. WT, wild type; DM, *hma2,hma4* double mutant. **a**, Zinc; **b**, magnesium; **c**, phosphorus; and **d**, manganese. Data are means \pm s.d. of eight to ten replicates, WT \times DM of three replicates. Statistical analysis indicates significant difference from the wild type ($*p < 0.01$).

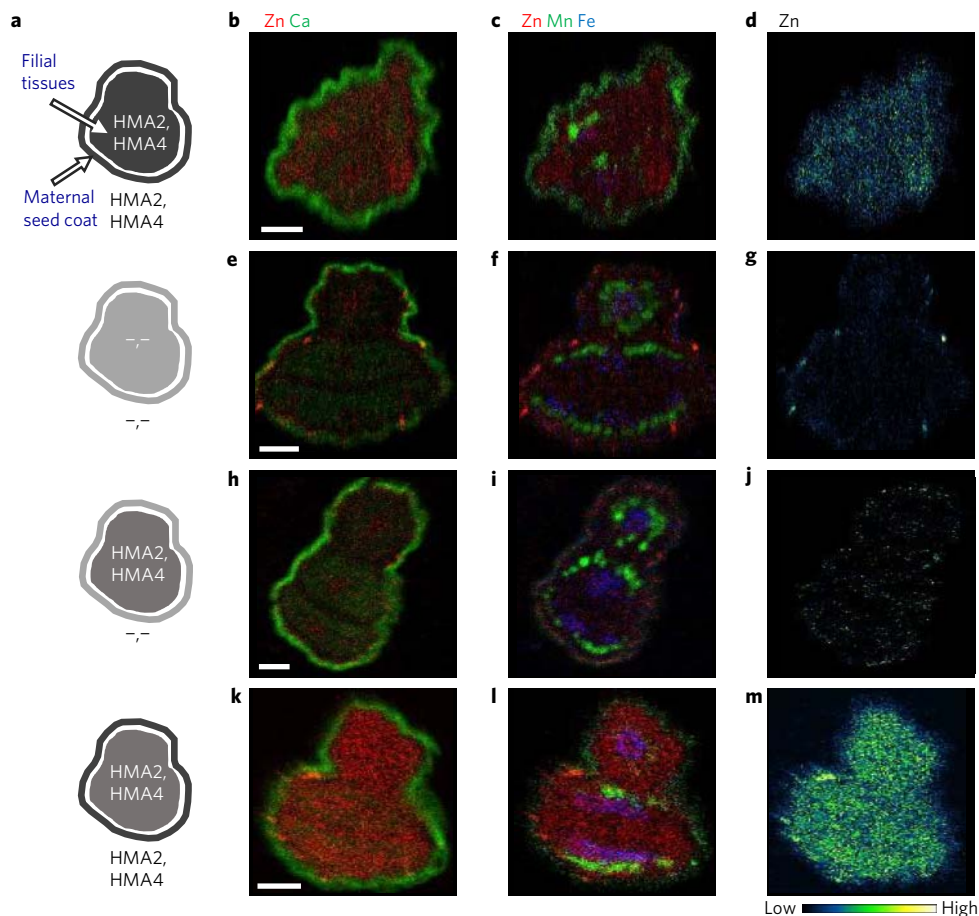


Figure 4 | Zinc export from the seed coat to filial tissues depends on zinc pumps in maternal tissues. μ PIXE/RBS elemental profiles of transverse sections of seeds from crosses of plants grown at high zinc supply. **a**, Pictograms indicate presence of AtHMA2 and AtHMA4. Dark grey, AtHMA2 and AtHMA4 present (homozygous WT); intermediate grey, AtHMA2 and AtHMA4 present (hemizygous); light grey, AtHMA2 and AtHMA4 absent (homozygous *hma2,hma4*). **b-m**, Colour maps showing distribution of elements. Two-colour maps showing zinc (Zn) distribution in red and calcium (Ca) distribution in green (**b,e,h,k**). Three-colour maps showing zinc (Zn) distribution in red, manganese (Mn) distribution in green and iron (Fe) distribution in blue (**c,f,i,l**). Temperature colour maps displaying zinc distribution (**d,g,j,m**). Scale bars, 50 μ m.

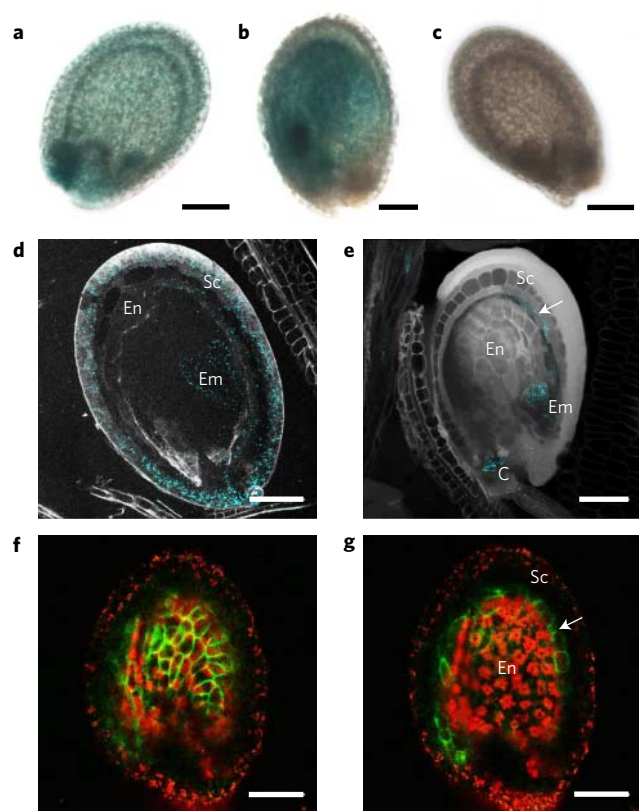


Figure 5 | *AtHMA2* and *AtHMA4* are expressed in developing seeds. **a–e**, Histochemical staining for GUS activity in developing seeds harbouring reporter gene fusions of the *AtHMA2* promoter (**a,d**) and *AtHMA4* promoter (**b,e**). (**c**) Wild-type seed. The images show whole seeds (**a–c**) and confocal laser scanning optical sections of modified pseudo-Schiff propidium iodide (mPS-PI)-stained seeds (**d,e**). **f–g**, Two different confocal laser scanning optical sections of the same developing seed expressing a fusion between a part of *AtHMA4* and GFP under the control of the *AtHMA4* promoter. Green, GFP fluorescence; red, autofluorescence; C, chalazal region; En, endosperm; Em, embryo; Sc, seed coat. The arrow indicates the endothelium. Scale bars, 100 μm .

1 correspond to the endothelium of the seed coat in *Arabidopsis*. The
 2 homologue in rice is OsHMA2, which functions as a zinc transporter
 3 involved in the root-to-shoot translocation of zinc^{23–25}. Whether
 4 HvHMA2 and OsHMA2 also play crucial roles in the developing
 5 grain remains to be investigated; however, it is conceivable that
 6 they would have similar functions as *AtHMA2–4*. In efforts to
 7 increase the zinc translocation capacity of plants, *HMA4* from
 8 either *A. thaliana* or *A. halleri* has been transgenically expressed
 9 in *Arabidopsis*, *Nicotiana tabacum* (tobacco) and *Solanum lycopersicum*
 10 (tomato), but with inconsistent results^{14,15,26–29}. Notably, none
 11 of these studies made use of endogenous *HMA* promoters. Cellular
 12 mislocalization of *HMA4* is likely to cause undesired export of zinc
 13 and interrupt the natural flow of zinc within the plant body. To
 14 attain this goal, the natural expression patterns of *HMA2* or
 15 *HMA4* should be retained. The finding that localization of
 16 *AtHMA4* to the seed coat endothelium is crucial for export of
 17 zinc into the seed provides us with an essential handle in breeding
 18 efforts aimed at fighting hidden hunger.

19 Methods

20 **Plant material.** *A. thaliana* Columbia-0 was used as the wild type. The single
 21 mutants *hma2-4* and *hma4-2* and the double mutant *hma2-4,hma4-2* were as
 22 described¹⁵. Plant growth, cloning and plant transformation procedures for creating
 23 transgenic GUS and GFP plants are described in the Supplementary Methods.

Multi-elemental analysis. Samples were prepared for multi-elemental analysis as
 24 described in the Supplementary Materials and Methods. Multi-elemental analysis of
 25 seeds was performed using flow injection analysis (FIA) with the following
 26 parameters: ICPMS was set up with an injection volume of 50 μl , a flow of
 27 0.2 ml min^{-1} and a mobile phase of 3.5% HNO_3 . For the FIA, a Thermo ICS
 28 5,000 DP pump and an Ultimate 3,000 UHPLC auto-sampler (Thermo Scientific)
 29 were used. A triple quad ICPMS (Model 8,800, Agilent Technologies) equipped with
 30 an Ari Mist HP nebulizer (Burgener Research International) was used. The ICPMS
 31 instrument was run in collision mode using helium as the collision gas; zinc,
 32 manganese, magnesium and phosphorus were analysed at m/z ratios of 66, 55, 24
 33 and 31, respectively. Data were acquired and processed using the MassHunter 4.1
 34 Chromatographic software package. For external calibration, a custom-made
 35 multi-element standard was used (P/N 4400-ICP-MSCS, CPI International). The
 36 standard is non-equimolar and corresponds to the ratio between elements typically
 37 found in plants. The digestion procedure and elemental analysis were validated using
 38 the certified reference material (CRM) NIST 1,515 Apple Leaf (National Institute
 39 of Standard and Technology). For magnesium, phosphorus, manganese and zinc,
 40 an accuracy of within $\pm 10\%$ was obtained for samples ranging in size from 200 to
 41 2,000 μg ($n = 8$). *Arabidopsis* seeds were analysed in sample batches of ten intact
 42 seeds or ten fractionated seeds divided into seed coats and embryos, typically
 43 weighing from 50 to 200 μg . The elemental concentrations in these small sample
 44 batches were reported as nanograms of element per ten seeds. The combined masses
 45 of the elements measured in the seed coat plus embryo were within $\pm 10\%$ of the
 46 masses determined in the whole seed, indicating a negligible level of sample loss or
 47 contamination during the analytical procedure. 48

$\mu\text{PIXE/RBS}$. Seeds were immersed in a droplet of resin (OCT, Tissue Teck Sakura)
 49 and immediately cryo-fixed by plunging into isopentane cooled with liquid nitrogen.
 50 Seed cross-sections (30 μm) were done using a cryo-microtome (Leica) and freeze-
 51 dried (48 h, -52°C , 0.01 mbar). Samples were analysed under vacuum at the Atomic
 52 Energy Commission nuclear microprobe (Saclay, France). The beamline was
 53 operated with a proton source at 3.03 MeV, with a beam focused to $3 \times 3 \mu\text{m}^2$ and a
 54 current intensity of 500 pA. 55

GUS analysis. Developing siliques were slit open longitudinally and stained for 3 h
 56 at 37°C in GUS staining solution following 5 min of vacuum treatment. The GUS
 57 staining solution contained 50 mM NaPO_4 at pH 7.2, 3 mM ferricyanide, 3 mM
 58 ferrocyanide, 0.4% Tween20 and 2 mM X-GlcA. The samples were then cleared in
 59 98% ethanol or fixed in fixing solution (50% methanol and 10% acetic acid) for
 60 modified pseudo-Schiff propidium iodide (mPS-PI) staining. The mPS-PI staining
 61 was as described³⁰. Samples were examined using a Leica TCS SP5X confocal
 62 microscope with a $20\times$ water immersion objective in sequential mode and were
 63 excited with a 488 nm argon laser. The propidium iodide emission signal was
 64 collected at 520–720 nm and the GUS reflection signal was collected at 485–491 nm
 65 (using the AOBs reflection mode). Cleared developing seeds were imaged by
 66 brightfield microscopy (Leica DM 5000B). 67

GFP analysis. To image developing seeds, siliques were slit open longitudinally and
 68 seeds were gently removed using a scalpel, mounted on a microscope slide and
 69 imaged immediately. Fluorescence microscopy was performed using an inverted
 70 point-scanning confocal microscope (Leica TCS SP5 II) with a $20\times$ water immersion
 71 objective. Samples were excited with a 488 nm argon laser; emission was collected at
 72 500–530 nm for GFP and at 660–700 nm for chlorophyll autofluorescence. 73

Received 17 February 2015; accepted 29 February 2016; 74

published xx xx 2016 75

References 76

- 77 Wessells, K. R. & Brown, K. H. Estimating the global prevalence of zinc
 78 deficiency: results based on zinc availability in national food supplies and the
 79 prevalence of stunting. *PLoS One* **7**, e50568 (2012).
- 80 von Grebmer, K. *et al.* *Global hunger index: the challenge of hidden hunger*
 81 (International Food Policy Research Institute, 2014).
- 82 Palmgren, M. G. *et al.* Zinc biofortification of cereals: problems and solutions.
 83 *Trends Plant Sci.* **13**, 464–473 (2008).
- 84 Stadler, R., Lauterbach, C. & Sauer, N. Cell-to-cell movement of green
 85 fluorescent protein reveals post-phloem transport in the outer integument and
 86 identifies symplastic domains in *Arabidopsis* seeds and embryos. *Plant Physiol.*
 87 **139**, 701–712 (2005).
- 88 Zhang, W. *et al.* Nutrient loading of developing seeds. *Funct. Plant Biol.* **34**,
 89 314–331 (2007).
- 90 Radchuk, V. & Borisjuk, L. Physical, metabolic and developmental functions of
 91 the seed coat. *Front. Plant Sci.* **5**, 510 (2014).
- 92 Williams, L. E. & Mills, R. F. P1B-ATPases – an ancient family of transition
 93 metal pumps with diverse functions in plants. *Trends Plant Sci.* **10**,
 94 491–502 (2005).
- 95 Baxter, I. *et al.* Genomic comparison of P-type ATPase ion pumps in
 96 *Arabidopsis* and rice. *Plant Physiol.* **132**, 618–628 (2003).

- 1 9. Kim, Y.-Y. *et al.* AtHMA1 contributes to the detoxification of excess Zn(II) in
2 *Arabidopsis*. *Plant J.* **58**, 737–753 (2009).
- 3 10. Seigneurin-Berny, D. *et al.* HMA1, a new Cu-ATPase of the chloroplast
4 envelope, is essential for growth under adverse light conditions. *J. Biol. Chem.*
5 **281**, 2882–2892 (2006).
- 6 11. Morel, M. *et al.* AtHMA3, a P(1B)-ATPase allowing Cd/Zn/Co/Pb vacuolar
7 storage in *Arabidopsis*. *Plant Physiol.* **149**, 894–904 (2009).
- 8 12. Hussain, D. *et al.* P-type ATPase heavy metal transporters with roles in essential
9 zinc homeostasis in *Arabidopsis*. *Plant Cell* **16**, 1327–1339 (2004).
- 10 13. Sinclair, S. A. *et al.* The use of the zinc-fluorophore, Zinpyr-1, in the study of
11 zinc homeostasis in *Arabidopsis* roots. *New Phytol.* **174**, 39–45 (2007).
- 12 14. Vernet, F. *et al.* Overexpression of AtHMA4 enhances root-to-shoot
13 translocation of zinc and cadmium and plant metal tolerance. *FEBS Lett.* **576**,
14 306–312 (2004).
- 15 15. Hanikenne, M. *et al.* Evolution of metal hyperaccumulation required *cis*-
16 regulatory changes and triplication of HMA4. *Nature* **453**, 391–396 (2008).
- 17 16. Kim, S. A. *et al.* Localization of iron in *Arabidopsis* seed requires the vacuolar
18 membrane transporter VIT1. *Science* **314**, 1295–1298 (2006).
- 19 17. Schnell Ramos, M. *et al.* Using μ PIXE for quantitative mapping of metal
20 concentration in *Arabidopsis thaliana* seeds. *Front Plant Sci.* **4**, 168 (2013).
- 21 18. Le, B. H. *et al.* Global analysis of gene activity during *Arabidopsis* seed
22 development and identification of seed-specific transcription factors. *Proc. Natl*
23 *Acad. Sci. USA* **107**, 8063–8070 (2010).
- 24 19. Song, W.-Y. *et al.* *Arabidopsis* PCR2 is a zinc exporter involved in both zinc
25 extrusion and long-distance zinc transport. *Plant Cell* **22**, 2237–2252 (2010).
- 26 20. Morth, J. P. *et al.* A structural overview of the plasma membrane Na⁺,K⁺-ATPase
27 and H⁺-ATPase ion pumps. *Nature Rev. Mol. Cell Biol.* **12**, 60–70 (2011).
- 28 21. Mills, R. F. *et al.* HvHMA2, a P1B-ATPase from barley, is highly
29 conserved among cereals and functions in Zn and Cd transport. *PLoS One* **7**,
30 e42640 (2012).
- 31 22. Tauris, B. *et al.* A roadmap for zinc trafficking in the developing barley grain
32 based on laser capture microdissection and gene expression profiling. *J. Exp. Bot.*
33 **60**, 1333–1347 (2009).
- 34 23. Satoh-Nagasawa, N. *et al.* Mutations in rice (*Oryza sativa*) Heavy Metal ATPase
35 2 (OsHMA2) restrict the translocation of zinc and cadmium. *Plant Cell Physiol.*
36 **53**, 213–224 (2012).
- 37 24. Takahashi, R. *et al.* The OsHMA2 transporter is involved in root-to-shoot
38 translocation of Zn and Cd in rice. *Plant Cell Environ.* **35**, 1948–1957 (2012).
- 39 25. Yamaji, N. *et al.* Preferential delivery of zinc to developing tissues in rice is
40 mediated by P-type heavy metal ATPase OsHMA2. *Plant Physiol.*
41 **162**, 927–939 (2013).
26. Barabasz, A. *et al.* Metal accumulation in tobacco expressing *Arabidopsis halleri*
42 metal hyperaccumulation gene depends on external supply. *J. Exp. Bot.* **61**,
43 3057–3067 (2010).
- 44 27. Siemianowski, O. *et al.* Expression of the P1B-type ATPase AtHMA4 in tobacco
45 modifies Zn and Cd root to shoot partitioning and metal tolerance. *Plant*
46 *Biotechnol. J.* **9**, 64–74 (2011).
- 47 28. Cun, P. *et al.* Modulation of Zn/Cd P1B2-ATPase activities in *Arabidopsis*
48 impacts differently on Zn and Cd contents in shoots and seeds. *Metallomics* **6**,
49 2109–2916 (2014).
- 50 29. Kendziorek, M. *et al.* Approach to engineer tomato by expression of AtHMA4 to
51 enhance Zn in the aerial parts. *J. Plant Physiol.* **171**, 1413–1422 (2014).
- 52 30. Truernit, E. *et al.* High-resolution whole-mount imaging of three-dimensional
53 tissue organization and gene expression enables the study of phloem
54 development and structure in *Arabidopsis*. *Plant Cell* **20**, 1494–1503 (2008).
- 55

Acknowledgements

The authors thank C.S. Cobbett (University of Melbourne) for providing *hma2-4*, *hma4-2*, and *hma2-4*, *hma4-2* mutant seeds and the Centre for Advanced Bioimaging (University of Copenhagen) for support and use of microscopes. We acknowledge the Paul Scherrer Institut, Villigen, Switzerland, for providing the synchrotron radiation beamtime at beamline MicroXAS of the SLS. The research leading to these results was funded by the University of Copenhagen's Excellency Programme KU2016, the People Programme (Marie Curie Actions) of the European Union's Seventh Framework Programme (FP7/2007-2013) under REA grant agreement no. PIEF-GA-2012-331680, and the European programme CALIPSO (no. 312284).

Author contributions

L.I.O., T.H.H., C.L., J.T.H., J.L., S.S., S.C. and V.S. performed the experimental work. L.I.O., T.H.H., C.L., R.D.H., J.L., S.S., U.K., S.H. and M.P. performed data analysis. D.G., U.K., S.H. and M.P. oversaw project planning. L.I.O. and M.P. wrote the manuscript. All authors discussed the results and commented on the manuscript.

Additional information

Supplementary information is available online. Reprints and permissions information is available online at www.nature.com/reprints. Correspondence and requests for materials should be addressed to M.P.

Competing interests

The authors declare no competing financial interests.

Journal: NPLANTS

Article ID: nplants-2016-36

Article Title: Mother plant-mediated pumping of zinc into the developing seed

Author(s): Lene Irene Olsen *et al.*

| Query Nos. | Queries | Response |
|------------|---|----------|
| 1 | For all author addresses, please provide post/zip code | |
| 2 | What does HMA stand for? | |
| 3 | Ref 17: Please provide final page number if article is greater than one page. | |
| 4 | Figure 4: please check edits to the caption | |